

# Number of Nuclear Divisions in the *Drosophila* Blastoderm Controlled by Onset of Zygotic Transcription

Hung-wei Sung,<sup>1</sup> Saskia Spangenberg,<sup>1</sup> Nina Vogt,<sup>2</sup> and Jörg Großhans<sup>1,\*</sup>

<sup>1</sup>Institut für Biochemie, Universitätsmedizin, Universität Göttingen, Justus-von-Liebig Weg 11, 37077 Göttingen, Germany

<sup>2</sup>Max Planck Institute for Developmental Biology, Spemannstrasse, 72076 Tübingen, Germany

## Summary

The cell number of the early *Drosophila* embryo is determined by exactly 13 rounds of synchronous nuclear divisions, allowing cellularization and formation of the embryonic epithelium [1]. The pause in G2 in cycle 14 is controlled by multiple pathways, such as activation of DNA repair checkpoint, progression through S phase, and inhibitory phosphorylation of Cdk1, involving the genes *grapes*, *mei41*, and *wee1* [2–8]. In addition, degradation of maternal RNAs [9] and zygotic gene expression [10, 11] are involved. The zinc finger *Vfl* controls expression of many early zygotic genes [12, 13], including the mitotic inhibitor *frühstart* [14, 15]. The functional relationship of these pathways and the mechanism for triggering the cell-cycle pause have remained unclear. Here, we show that a novel single-nucleotide mutation in the 3' UTR of the *RPII215* gene leads to a reduced number of nuclear divisions that is accompanied by premature transcription of early zygotic genes and cellularization. The reduced number of nuclear divisions in mutant embryos depends on the transcription factor *Vfl* and on zygotic gene expression, but not on *grapes*, the mitotic inhibitor *Frühstart*, and the nucleocytoplasmic ratio. We propose that activation of zygotic gene expression is the trigger that determines the timely and concerted cell-cycle pause and cellularization.

## Results and Discussion

Embryos from germline clones of the lethal mutation X161 (in the following, designated as mutant embryos) showed a reduced cell number but otherwise developed apparently normally until at least gastrulation stage (Figures 1A and 1B; 24 of 61 embryos). Cell specification along the anterior-posterior and dorsoventral axes proceeded as in wild-type, as demonstrated by the seven stripes of *eve* expression, mesoderm invagination, and cephalic furrow formation. The reduced cell number can be due to a lower number of nuclear divisions prior to cellularization or to loss of nuclei in the blastoderm. To distinguish these possibilities, we performed time-lapse recordings of mutant embryos in comparison to wild-type (Figure 1C and Table 1). To measure the cell-cycle length, we fluorescently labeled the nuclei in these embryos. We observed three types of embryos: (1) with 13 nuclear divisions with an extended interphase 13 (28 min versus 21 min in wild-type), (2) with 12 nuclear divisions, and (3) with partly 12

and partly 13 nuclear divisions with an extended interphase 13. Because we did not observe a severe nuclear fallout phenotype, we conclude that the reduced cell number in gastrulating embryos is due to the reduced number of nuclear divisions. Consistent with these observations, the number of centrosomes and centrosomes was normal in mutant embryos (see Figure S1 available online).

In wild-type embryos, interphase 14 is different from the preceding interphases, in that the plasma membrane invaginates to enclose the individual nuclei into cells. In X161 embryos with patches in nuclear density, furrow markers showed more advanced furrows in the part with a lower number of divisions, indicating a premature onset of cellularization (Figure 1D). Furthermore, in time-lapse recordings, we first measured the speed of membrane invagination, finding no obvious difference between X161 and wild-type embryos (Figure S1). Additionally, we investigated cellularization by live imaging with moesin-GFP labeling F-actin (Figure 1E). Clear accumulation of F-actin at the furrow canals was observed in wild-type embryos after about 20 min in interphase 14, but not in interphase 13. In X161 embryos with 12 nuclear divisions, we observed a comparable reorganization already in interphase 13 after about 25 min. This analysis shows that both the cell-cycle pause and cellularization are initiated in X161 embryos earlier than in wild-type embryos.

To identify the mutated gene in X161, we mapped the lethality and blastoderm phenotype (Figure S2). The X161 gene was separated from associated mutations on the chromosome by meiotic recombination and mapped to a region of four genes by complementation analysis with duplications and deficiencies. Sequencing of the mapped region and complementation tests with two independent *RPII215* loss-of-function alleles, *RPII215*[1] and *RPII215*[G0040] [16, 17], and a transgene comprising the *RPII215* locus revealed the large subunit of the RNA polymerase II as the mutated gene. We identified a single point mutation in the 3' UTR of *RPII215* about 40 nt downstream of the stop codon. This region in the 3' UTR is not conserved and does not show any obvious motifs (Figure S2).

To test whether the mutation in the noncoding region affects transcript or protein expression, we quantified mRNA levels by reverse transcription and quantitative PCR and protein levels by whole-mount staining and immunoblotting with extracts of manually staged embryos. We found that mRNA levels were not different in wild-type and X161 (Figure 2A and Table S1). In contrast, immunohistology and immunoblotting revealed reduced RPII215 protein levels (Figures 2B and 2C). In summary, our analysis shows that the X161 point mutation within the 3' UTR affects mainly RPII215 protein levels.

The precocious onset of cellularization raised the hypothesis that the timing of zygotic gene expression may be affected in the X161 embryos. To establish the expression profiles of selected maternal and zygotic genes, we employed nCounter NanoString technology [18] with embryos staged by the nuclear division cycle (Figure S3 and Table S2). Embryos expressing histone 2Av-RFP were manually selected 3 min after anaphase of the previous mitosis or at midcellularization. We first analyzed expression of ribosomal proteins (Figure S3).

\*Correspondence: [jgrossh@gwdg.de](mailto:jgrossh@gwdg.de)



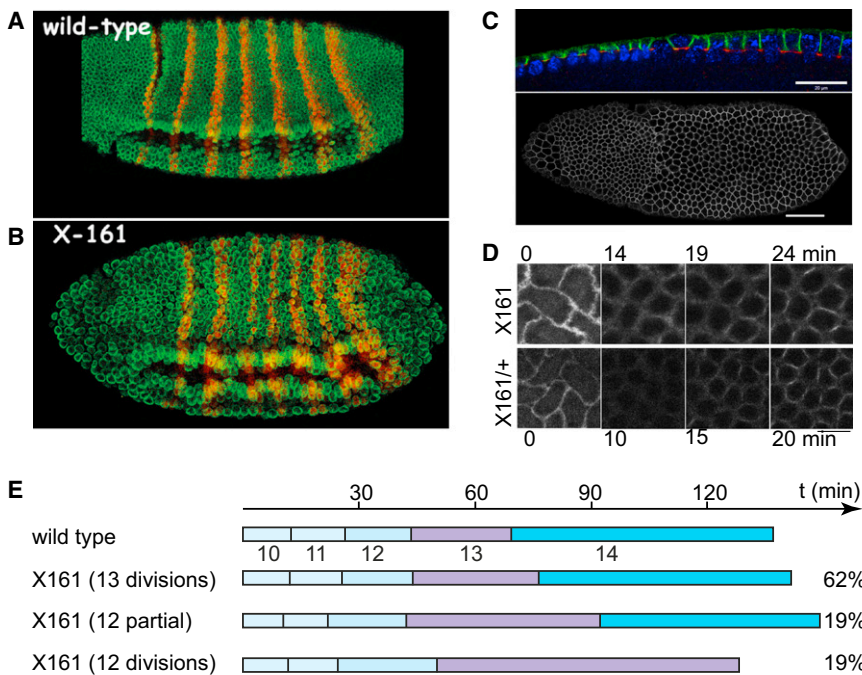


Figure 1. Reduced Number of Nuclear Divisions in X161 Embryos

(A–C) Fixed wild-type (A) and X161 (B and C) embryos were stained for pair-rule protein Eve (red) and the nuclear lamina protein Kuk (green) (A and B) or for Slam (red), Dlg (green, white), and DNA (blue) (C). Scale bars represent 20  $\mu\text{m}$  and 50  $\mu\text{m}$ .

(D) Images from time-lapse recording of X161 or X161/+ embryos expressing moesin-GFP to label F-actin accumulation at the metaphase furrow and emerging furrow canal. Scale bar represents 10  $\mu\text{m}$ .

(E) Cell-cycle lengths. X161 embryos were classified according to the behavior in cycle 13 with complete, partial, and absent mitosis 13. The numbers on the right hand side of the bars indicate the proportion of the embryos with this phenotype.

They did not change much and were not different in wild-type and mutant embryos, confirming the robustness of the method. Zygotic genes, whose expression strongly increases during the syncytial cycles, showed an earlier upregulation in X161 than in wild-type embryos (Figure 3A). Comparing the profiles by plotting the ratio of the expression levels (Figure 3B), we revealed a clear difference in cycle 12, with a factor of up to ten, indicating that zygotic genes are precociously expressed in X161 embryos. The premature expression of early zygotic genes was confirmed by whole-mount in situ hybridization for *slam* and *frs* mRNA (Figure S4).

Next, we analyzed expression profiles of RNAs subject to RNA degradation. We selected transcripts representative for the two classes of degradation, depending on zygotic gene expression (Figure 3C), and on egg activation (Figure S3) [19–23]. Degradation of *string*, *twine*, and *smaug* transcripts in interphase 14 depends of zygotic gene expression. In X161 mutants, the mRNA of these three genes was degraded already in cycle 13, slightly sooner than in wild-type (Figure 3C). The profiles of *string* and *twine* RNA were confirmed by RNA in situ hybridization (Figure S4). Consistent with the

precocious RNA degradation in X161, *Twine* and *String* protein levels decreased already in interphase 13 of X161 embryos (Figure 3D).

Finally, we analyzed the profile of mRNAs whose degradation depends on egg activation (Figure S4). We did not detect a consistent pattern and a clear difference between the profiles of wild-type and X161 mutants. Our data show that zygotic gene expression starts earlier in X161 than in wild-type and that degradation of mRNAs follows zygotic gene expression.

The cell cycle may be paused prematurely by altered levels of maternal factors, such as *CyclinB*, *grapes*, and *twine*, or by precociously expressed zygotic genes, such as *frs* and *trbl* [14, 15, 24]. To distinguish these two options, we analyzed mutant embryos with suppressed zygotic gene expression (Figures 4A and 4B). Embryos injected with the RNA polymerase II inhibitor  $\alpha$ -amanitin develop until mitosis 13 but then fail to cellularize and may undergo an additional nuclear division, depending on injection conditions [10, 25]. Using this assay, we tested whether zygotic genes are required for the reduced number of nuclear divisions in X161 mutants. If the precocious cell-cycle pause were due, for example, to reduced levels of *CyclinB* mRNA,  $\alpha$ -amanitin injection should not change the reduced number of divisions. We observed that all injected mutant embryos passed through at least 13 nuclear divisions, similar to injected wild-type embryos, whereas injection of water resulted in a mixed phenotype of 12 and 13 nuclear

Table 1. Reduced Number of Nuclear Divisions in X161 Mutants

Genotype	Pause after	n	Cell Cycle (Length in Minutes)				
			10	11	12	13	14
Wild-type	13	18	9.9 $\pm$ 1.1	12.2 $\pm$ 1	14.8 $\pm$ 1.1	21.1 $\pm$ 2.5	57.1 $\pm$ 4.4
X161	13	8	10.6 $\pm$ 0.9	11.8 $\pm$ 1	15.1 $\pm$ 1.9	28 $\pm$ 2.3	55.4 $\pm$ 8.7
X161	12/13	3	9	9.7 $\pm$ 0.5	17 $\pm$ 2	41.8 $\pm$ 4.4	48.2 $\pm$ 9.5
X161	12	3	10	11 $\pm$ 1	12 $\pm$ 4.5	66 $\pm$ 12	
<i>vfl</i>	13	6	8 $\pm$ 1.4	11.6 $\pm$ 2.6	13.6 $\pm$ 0.9	22 $\pm$ 1.4	– <sup>a</sup>
<i>vfl</i>	14	2	7	9	17	22	28
X161 <i>vfl</i>	13	6	10.3 $\pm$ 1.3	10.5 $\pm$ 5.4	15.8 $\pm$ 6.7	30 $\pm$ 12.8	– <sup>a</sup>
X161 <i>vfl</i>	14	4	9	13 $\pm$ 2.8	10 $\pm$ 1	14 $\pm$ 1	30 $\pm$ 5.2

<sup>a</sup>*vfl* and X161 *vfl* embryos do not cellularize and have no zygotically controlled mitosis corresponding to mitosis 14 in wild-type embryos. The given error represents SD.

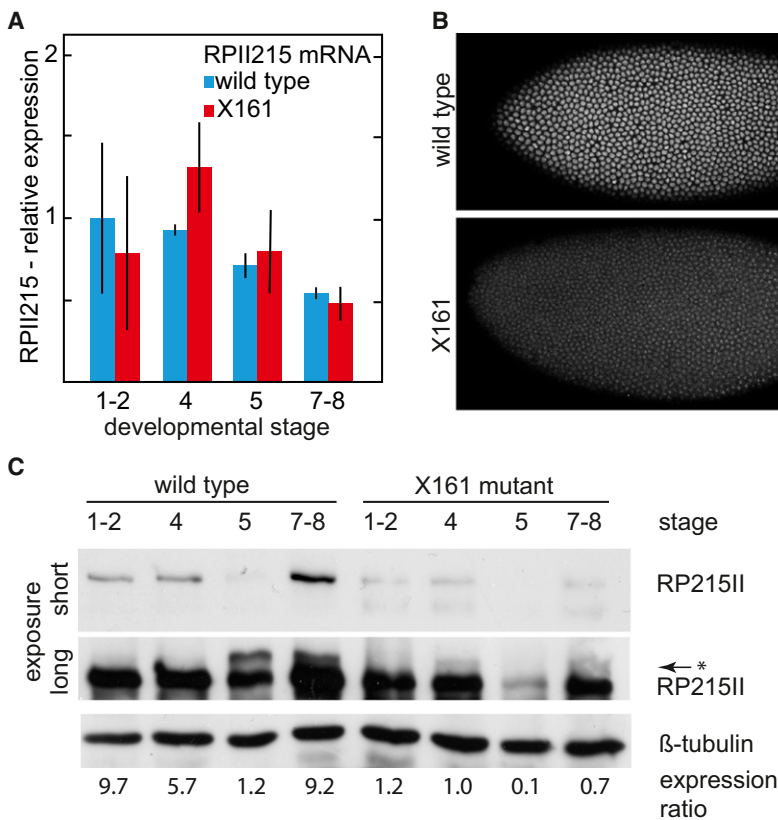


Figure 2. Expression of RPII215

(A) *RPII215* mRNA expression by RT-PCR. Error bars show quantification from three independent RNA samples. Expression levels were normalized to levels of 18S rRNA and related to expression in wild-type embryos in stage 1–2. Error bars represent SD.

(B) Fixed wild-type and X161 embryos stained for RPII215.

(C) Immunoblots of extracts from staged embryos as indicated with short and long exposures for RPII215 and  $\beta$ -tubulin. Expression (indicated by the numbers at the bottom) estimated by normalization to the tubulin bands (in a weak exposure film, not shown). Asterisk with arrow marks the activated form of RPII215.

divisions, comparable to uninjected X161 embryos (Figure 4B and Table 2). This experiment demonstrates that the reduced division number in X161 embryos requires zygotic gene expression.

The expression of many early zygotic genes is controlled by the zinc-finger protein Vfl (also called Zelda) [13]. We tested whether the precocious cell-cycle pause in X161 mutants is mediated by *vfl*-dependent genes. Analysis of X161 *vfl* double-mutant embryos revealed that, in contrast to X161 mutants, the cell cycle undergoes at least 13 divisions (Table 2). We further analyzed activation of zygotic gene expression by staining for Vfl and activated RPII215 (Figure S1). We detected staining of both in presyncytial stages of X161 mutants already in cycle 5. No specific staining for the activated RPII215 was detected in X161 *vfl* double-mutant embryos, and no difference in Vfl staining in syncytial embryos was detected in wild-type and X161 embryos (Figure S1). These findings show that the genes relevant for the precocious cell-cycle pause in X161 mutants are *vfl* target genes.

A zygotic gene involved in cell-cycle control is *frs*, which is sufficient to induce a pause of the cell cycle [15, 24]. Analysis of X161 *frs* double-mutant embryos showed, however, that the number of nuclear divisions was not changed as compared to X161 single mutants (Table 2). This indicates that *frs* is not the only cell-cycle inhibitor expressed in the early embryo.

Proteins mediating the DNA repair checkpoint, such as Grapes/Chk1, are required for the cell-cycle pause [2–8]. Passing normally through the nuclear division cycles, the cell cycle shows striking abnormalities in nuclear envelope formation and chromosome condensation in interphase 14 in embryos from *grapes* females. We tested whether the timing of the transition in cell-cycle behavior in *grapes* embryos

depends on the onset of zygotic transcription by analyzing X161 *grapes* double-mutant embryos (Figure 4D and Table 2). We found that some of the X161 *grapes* double mutants showed the defects in nuclear envelope formation and chromatin condensation already in interphase 13, indicating that the requirement of *grapes* for chromatin structure shifted from interphase 14 to 13. These data suggest that the activation of *grapes* and the DNA checkpoint depends on the onset of zygotic gene expression.

A factor controlling the number of nuclear divisions is the ploidy of the embryo, given that haploid embryos undergo 14 instead of 13 nuclear divisions prior to cellularization [1, 26]. Based on this and on related observations, it has been proposed that the nucleocytoplasmic (N/C) ratio controls the trigger for MBT. To address the functional relationship of X161 and the N/C ratio, we analyzed haploid X161 embryos (Figure 4E and Table 2). We observed a mixture in the number of nuclear divisions between 12 and 14 in fixed embryos. We even observed embryos containing three patches with nuclear densities corresponding to 12, 13, and 14 nuclear divisions (Figures 4F and 4G). About half of the embryos underwent 12 nuclear divisions, similar to X161 embryos. These data suggest that ploidy acts independently of general onset of zygotic transcription, which is consistent with the observation that only a subset of zygotic genes are expressed with a delay in haploid embryos [27]. Consistent with this report, cellularization starts for a first time temporarily in interphase 14 in haploid embryos and for a second time in interphase 15. These observations suggest that the N/C ratio in *Drosophila* specifically affects cell-cycle regulators such as *frs*, for example, but not general zygotic genome activation and onset of cellularization.

In summary, our data support the model that activation of the zygotic genome controls the timing of the MBT. First, onset of MBT is sensitive to changes in RNA polymerase II activity. Second, the changes in zygotic gene expression in X161 embryos occur earlier than the changes in zygotic RNA degradation, Cdc25 protein destabilization, or activation of *grapes*. Third, the X161 mutant phenotype depends on zygotic transcription and on the transcription factor Vfl, showing that the precocious cell-cycle pause and onset of cellularization

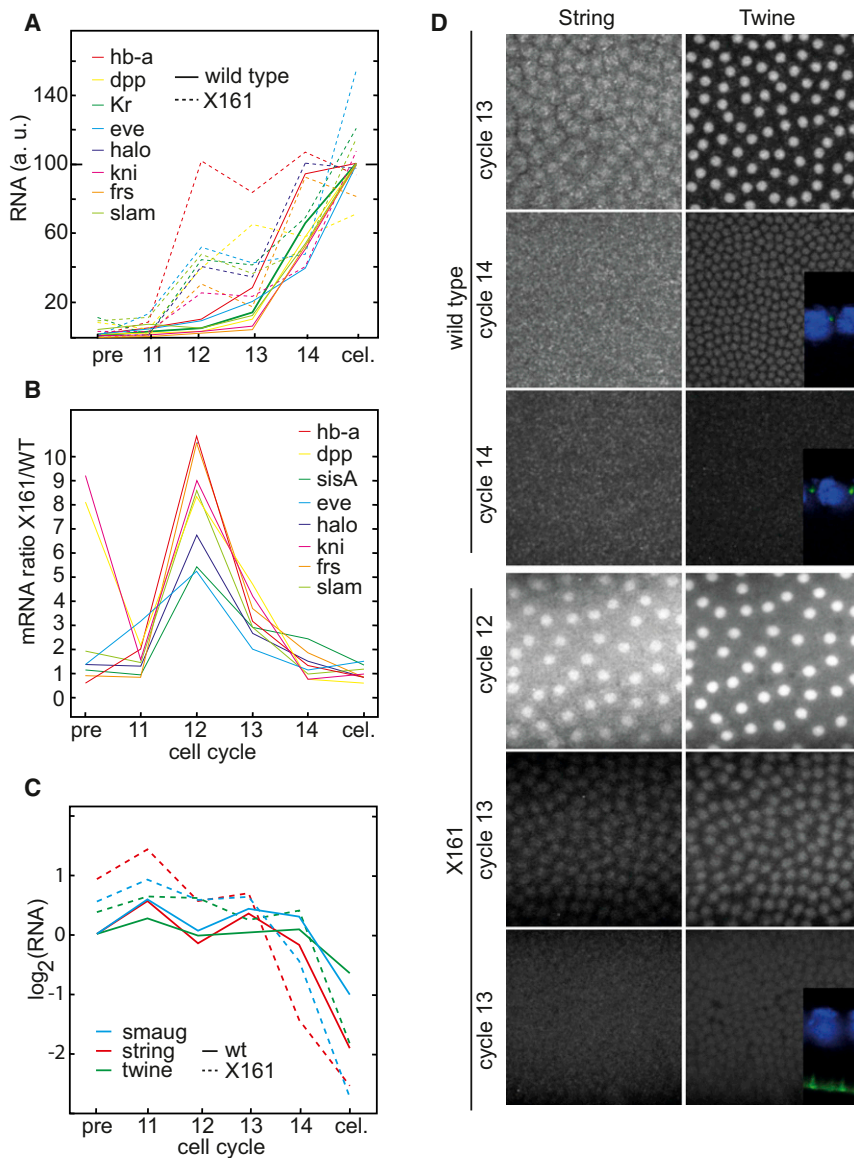


**Figure 3. Expression Profiles of Zygotic and Maternal Genes**

(A–C) Transcript levels in staged embryonic extracts measured by NanoString technology. “pre,” presyncytial cycles 1–8; 11, 12, 13, 14, number of interphase; “cel,” embryos in cellularization when the furrow is at the basal side of the nuclei in interphase 14 in wild-type embryos and in interphase 13 in X161 embryos.

(A) Profiles of zygotic genes, normalized to expression level at “cel” in wild-type embryos.

(B) Ratio of expression levels of the indicated genes in X161 and wild-type embryos. Note that the readings at early stage were very low and at the background levels. Please see [Supplemental Information](#) for the numbers.

(C) *string*, *twine*, and *smaug* mRNA levels in wild-type embryos (solid lines) and X161 embryos (dashed lines); y axis in log<sub>2</sub>. Expression levels are relative to the expression level in wild-type presyncytial embryos.

(D) Wild-type and X161 embryos stained for String and Twine proteins. The inset shows Slam and DNA staining to indicate the progression of cellularization.

cannot be due to changes in maternal factors, such as higher expression of *CyclinB*. Although the altered levels of RNA polymerase II in X161 mutants probably affect expression of many genes during oogenesis, these changes seem not to matter in functional terms, given the overall normal morphology and specific mutant phenotype. It is conceivable that transcriptional repressors are expressed or translated in eggs in lower levels. In the embryo, such lower levels of repressors would allow the trigger for onset of zygotic gene expression to reach the threshold earlier than in wild-type embryos. The first signs of zygotic transcription are detected already during the presyncytial stages, before nuclear cycle 8/9. This may be the time when the trigger for MBT is activated.

#### Experimental Procedures

Genetic markers, strains, and genome annotation were according to Flybase (<http://flybase.org>). X161 was selected from a set of mutations in germline clones with defects in oogenesis and early embryogenesis [28]. Microinjection, RT-PCR, protein analysis, histological procedures, and live imaging were essentially as previously described [29–31]. Gene expression

levels in embryos manually staged by the nuclear division was determined by NanoString technology [18].

#### Supplemental Information

Supplemental Information includes four figures, two tables, and Supplemental Experimental Procedures and can be found with this article online at <http://dx.doi.org/10.1016/j.cub.2012.12.013>.

#### Acknowledgments

We thank S. Heidmann, C. Rushlow, S. Di Talia, the Developmental Studies Hybridoma Bank at the University of Iowa, and the Bloomington Drosophila Stock Center at Indiana University for materials and fly stocks. We thank A. Brandt and lab members for help with experiments. This work was in part supported by the German Research Council (DFG). H.-w.S. was in part supported by the German Academic Exchange Service (DAAD). N.V. was in part supported by the Boehringer Ingelheim Fonds.

Received: August 16, 2012

Revised: November 25, 2012

Accepted: December 10, 2012

Published: January 3, 2013

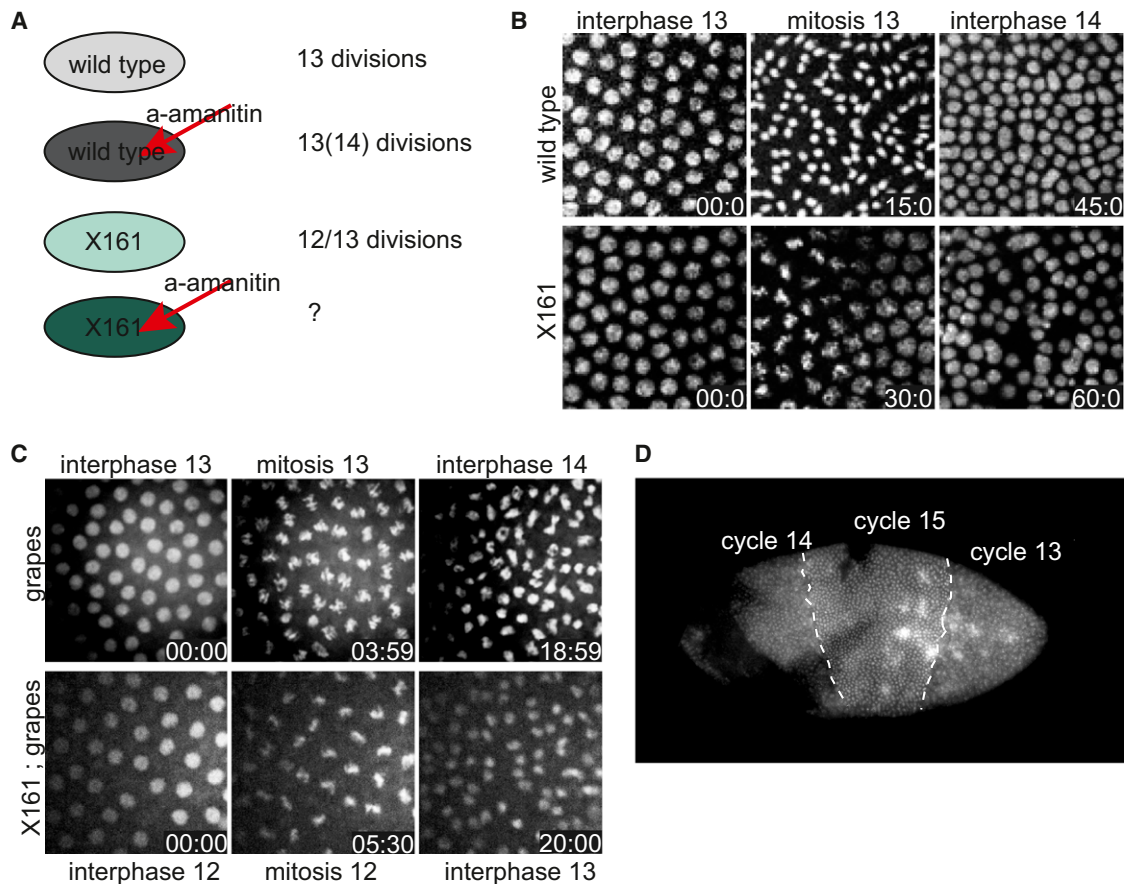


Figure 4. Reduced Number of Divisions Depends on Zygotic Gene Expression Controlled by *vfl*

(A) Experimental scheme of the  $\alpha$ -amanitin injection experiment. Wild-type embryos injected with  $\alpha$ -amanitin undergo 13 or 14 nuclear divisions, depending on conditions.  
 (B) Number of nuclear divisions is scored in injected wild-type and X161 mutant embryos expressing His2AvGFP. Temperature was 18°C–20°C.  
 (C) Images from time-lapse recordings of embryos from *grapes* and X161; *grapes* females injected with labeled histone1 during indicated cell cycle. *grapes* embryos show abnormal chromatin condensation in interphase 14.  
 (D) Fixed haploid X161 embryo stained for DNA. Regions with respective nuclear densities are marked.

## References

- Foe, V.E., Odell, G.M., and Edgar, B.A. (1993). Mitosis and morphogenesis in the *Drosophila* embryo. In *The Development of Drosophila melanogaster*, M. Bate and A. Martinez-Arias, eds. (Cold Spring Harbor, NY: Cold Spring Harbor Laboratory Press), pp. 149–300.
- Fogarty, P., Campbell, S.D., Abu-Shumays, R., Phalle, B.S., Yu, K.R., Uy, G.L., Goldberg, M.L., and Sullivan, W. (1997). The *Drosophila* *grapes* gene is related to checkpoint gene *chk1/rad27* and is required for late syncytial division fidelity. *Curr. Biol.* 7, 418–426.
- Sibon, O.C., Stevenson, V.A., and Theurkauf, W.E. (1997). DNA-replication checkpoint control at the *Drosophila* midblastula transition. *Nature* 388, 93–97.
- Sibon, O.C., Laurençon, A., Hawley, R., and Theurkauf, W.E. (1999). The *Drosophila* ATM homologue *Mei-41* has an essential checkpoint function at the midblastula transition. *Curr. Biol.* 9, 302–312.
- Royou, A., McCusker, D., Kellogg, D.R., and Sullivan, W. (2008). *Grapes*(*Chk1*) prevents nuclear CDK1 activation by delaying cyclin B nuclear accumulation. *J. Cell Biol.* 183, 63–75.
- Price, D., Rabinovitch, S., O'Farrell, P.H., and Campbell, S.D. (2000). *Drosophila* *wee1* has an essential role in the nuclear divisions of early embryogenesis. *Genetics* 155, 159–166.
- Stumpff, J., Duncan, T., Homola, E., Campbell, S.D., and Su, T.T. (2004). *Drosophila* *Wee1* kinase regulates Cdk1 and mitotic entry during embryogenesis. *Curr. Biol.* 14, 2143–2148.
- McClelland, M.L., Shermoen, A.W., and O'Farrell, P.H. (2009). DNA replication times the cell cycle and contributes to the mid-blastula transition in *Drosophila* embryos. *J. Cell Biol.* 187, 7–14.
- Bashirullah, A., Halsell, S.R., Cooperstock, R.L., Kloc, M., Karaiskakis, A., Fisher, W.W., Fu, W., Hamilton, J.K., Etkin, L.D., and Lipshitz, H.D. (1999). Joint action of two RNA degradation pathways controls the timing of maternal transcript elimination at the midblastula transition in *Drosophila melanogaster*. *EMBO J.* 18, 2610–2620.
- Edgar, B.A., Kiehle, C.P., and Schubiger, G. (1986). Cell cycle control by the nucleocytoplasmic ratio in early *Drosophila* development. *Cell* 44, 365–372.
- Merrill, P.T., Sweeton, D., and Wieschaus, E. (1988). Requirements for autosomal gene activity during precellular stages of *Drosophila melanogaster*. *Development* 104, 495–509.
- Staudt, N., Fellert, S., Chung, H.-R., Jäckle, H., and Vorbrüggen, G. (2006). Mutations of the *Drosophila* zinc finger-encoding gene *vielfältig* impair mitotic cell divisions and cause improper chromosome segregation. *Mol. Biol. Cell* 17, 2356–2365.
- Liang, H.L., Nien, C.Y., Liu, H.Y., Metzstein, M.M., Kirov, N., and Rushlow, C. (2008). The zinc-finger protein *Zelda* is a key activator of the early zygotic genome in *Drosophila*. *Nature* 456, 400–403.
- Grosshans, J., and Wieschaus, E. (2000). A genetic link between morphogenesis and cell division during formation of the ventral furrow in *Drosophila*. *Cell* 101, 523–531.

Table 2. Cell-Cycle Pause in X161 Depends on *vfl*

Genotype	Nuclear Divisions		
	12 <sup>a</sup>	13	14 <sup>b</sup>
OrR	0	128	0
OrR + $\alpha$ -amanitin	0	6	0
X161 + water	5	4	0
X161 + $\alpha$ -amanitin	0	23	1
X161	29	27	0
<i>vfl</i>	0	5	2
X161 <i>vfl</i>	0	5	4
<i>grapes</i>	0	14	-
X161; <i>grapes</i>	8	2	-
X161; Df <i>frs</i>	47	48	0
Haploid X161 <sup>c</sup>	19	11	6

<sup>a</sup>Including partial 13<sup>th</sup> division.

<sup>b</sup>Including partial 14<sup>th</sup> division.

<sup>c</sup>X161 germline clones crossed to ms(3)K81 males.

30. Wenzl, C., Yan, S., Laupsien, P., and Grosshans, J. (2010). Localization of RhoGEF2 during *Drosophila* cellularization is developmentally controlled by Slam. *Mech. Dev.* 127, 371–384.
31. Kanesaki, T., Edwards, C.M., Schwarz, U.S., and Grosshans, J. (2011). Dynamic ordering of nuclei in syncytial embryos: a quantitative analysis of the role of cytoskeletal networks. *Integr Biol (Camb)* 3, 1112–1119.
15. Grosshans, J., Müller, H.A., and Wieschaus, E. (2003). Control of cleavage cycles in *Drosophila* embryos by frühstart. *Dev. Cell* 5, 285–294.
16. Brickley, W.J., and Greenleaf, A.L. (1995). Functional studies of the carboxy-terminal repeat domain of *Drosophila* RNA polymerase II in vivo. *Genetics* 140, 599–613.
17. Meller, V.H., and Rattner, B.P. (2002). The roX genes encode redundant male-specific lethal transcripts required for targeting of the MSL complex. *EMBO J.* 21, 1084–1091.
18. Geiss, G.K., Bumgarner, R.E., Birditt, B., Dahl, T., Dowidar, N., Dunaway, D.L., Fell, H.P., Ferree, S., George, R.D., Grogan, T., et al. (2008). Direct multiplexed measurement of gene expression with color-coded probe pairs. *Nat. Biotechnol.* 26, 317–325.
19. Benoit, B., He, C.H., Zhang, F., Votruba, S.M., Tadros, W., Westwood, J.T., Smibert, C.A., Lipshitz, H.D., and Theurkauf, W.E. (2009). An essential role for the RNA-binding protein Smaug during the *Drosophila* maternal-to-zygotic transition. *Development* 136, 923–932.
20. De Renzis, S., Elemento, O., Tavazoie, S., and Wieschaus, E.F. (2007). Unmasking activation of the zygotic genome using chromosomal deletions in the *Drosophila* embryo. *PLoS Biol.* 5, e117.
21. Tadros, W., Goldman, A.L., Babak, T., Menzies, F., Vardy, L., Orr-Weaver, T., Hughes, T.R., Westwood, J.T., Smibert, C.A., and Lipshitz, H.D. (2007). SMAUG is a major regulator of maternal mRNA destabilization in *Drosophila* and its translation is activated by the PAN GU kinase. *Dev. Cell* 12, 143–155.
22. Bushati, N., Stark, A., Brennecke, J., and Cohen, S.M. (2008). Temporal reciprocity of miRNAs and their targets during the maternal-to-zygotic transition in *Drosophila*. *Curr. Biol.* 18, 501–506.
23. Thomsen, S., Anders, S., Janga, S.C., Huber, W., and Alonso, C.R. (2010). Genome-wide analysis of mRNA decay patterns during early *Drosophila* development. *Genome Biol.* 11, R93.
24. Gawliński, P., Nikolay, R., Goursot, C., Lawo, S., Chaurasia, B., Herz, H.M., Kussler-Schneider, Y., Ruppert, T., Mayer, M., and Grosshans, J. (2007). The *Drosophila* mitotic inhibitor Frühstart specifically binds to the hydrophobic patch of cyclins. *EMBO Rep.* 8, 490–496.
25. Edgar, B.A., and Datar, S.A. (1996). Zygotic degradation of two maternal Cdc25 mRNAs terminates *Drosophila*'s early cell cycle program. *Genes Dev.* 10, 1966–1977.
26. Pritchard, D.K., and Schubiger, G. (1996). Activation of transcription in *Drosophila* embryos is a gradual process mediated by the nucleocytoplasmic ratio. *Genes Dev.* 10, 1131–1142.
27. Lu, X., Li, J.M., Elemento, O., Tavazoie, S., and Wieschaus, E.F. (2009). Coupling of zygotic transcription to mitotic control at the *Drosophila* mid-blastula transition. *Development* 136, 2101–2110.
28. Vogt, N., Koch, I., Schwarz, H., Schnorrer, F., and Nüsslein-Volhard, C. (2006). The gammaTuRC components Grip75 and Grip128 have an essential microtubule-anchoring function in the *Drosophila* germline. *Development* 133, 3963–3972.
29. Großhans, J., Bergmann, A., Haffter, P., and Nüsslein-Volhard, C. (1994). Activation of the kinase Pelle by Tube in the dorsoventral signal transduction pathway of *Drosophila* embryo. *Nature* 372, 563–566.

**Current Biology, Volume 23  
Supplemental Information**

**Number of Nuclear Divisions  
in the *Drosophila* Blastoderm Controlled  
by Onset of Zygotic Transcription**

**Hung-wei Sung, Saskia Spangenberg, Nina Vogt, and Jörg Großhans**

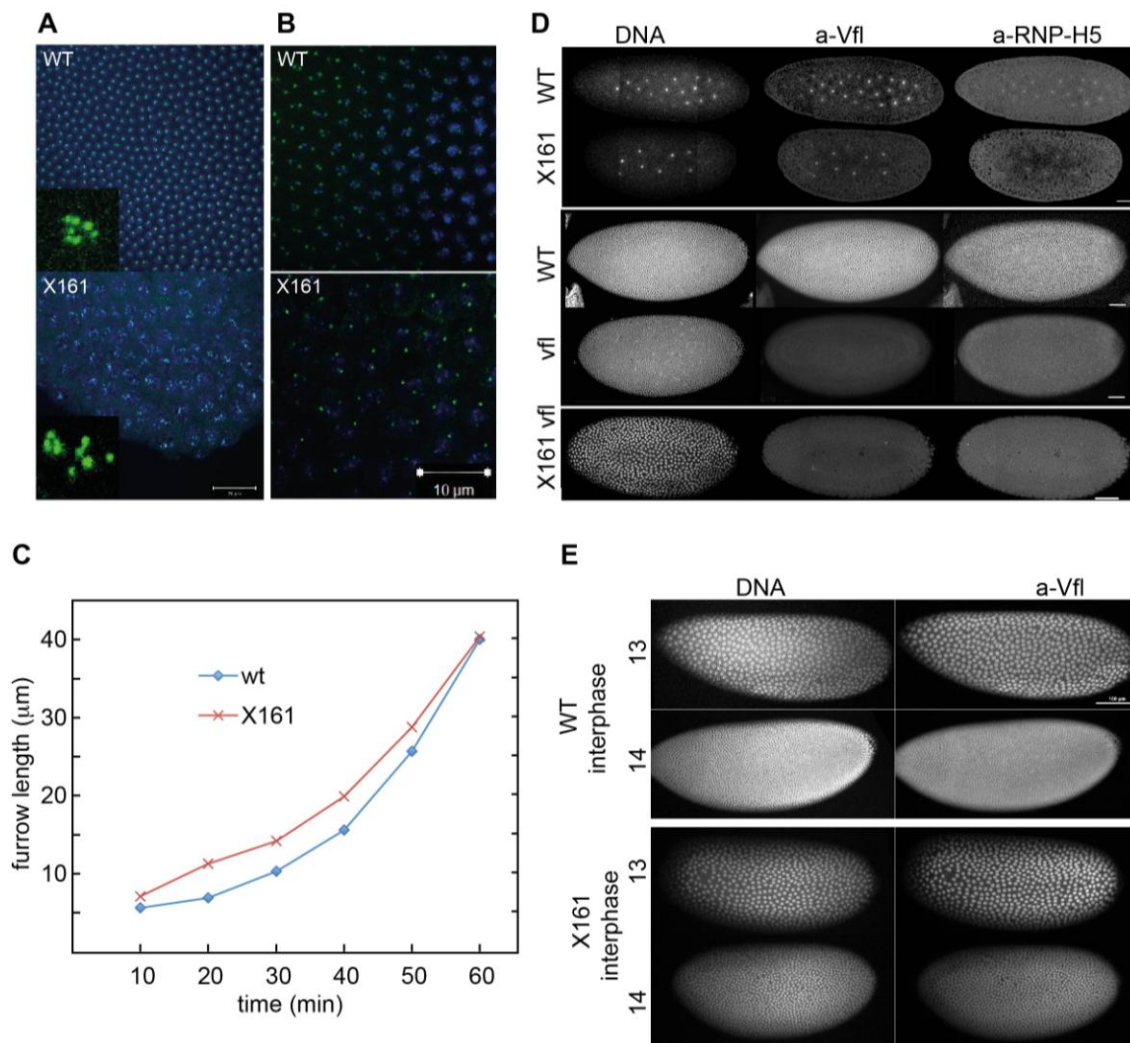


**Figure S1. X161 Phenotype, Vfl Expression and RPII215 Activity**

(A and B) Wild type and X161 embryos stained for the centromere protein Cid (green), DNA (blue) (A) or centrosomal protein gamma-tubulin (green) and DNA (blue) (B). Scale bars 10 μm. Insets in A show centromere staining in higher magnification.

(C) Progression of cellularisation in wild type and X161 embryos measured by the length of the furrow.

(D) Fixed wild type embryos and embryos from X161, *vfl* and X161 *vfl* germline clones as indicated were stained for DNA, Vfl, and RPII215-H5 (CTD phosphorylated form). Wild type embryos were marked with a histone-GFP transgene. Scale bar 50 μm.

(E) Fixed wild type embryos and embryos from X161 germline clones were stained for Vfl and DNA as indicated. Stage by cell cycle number was determined by the nuclear density.



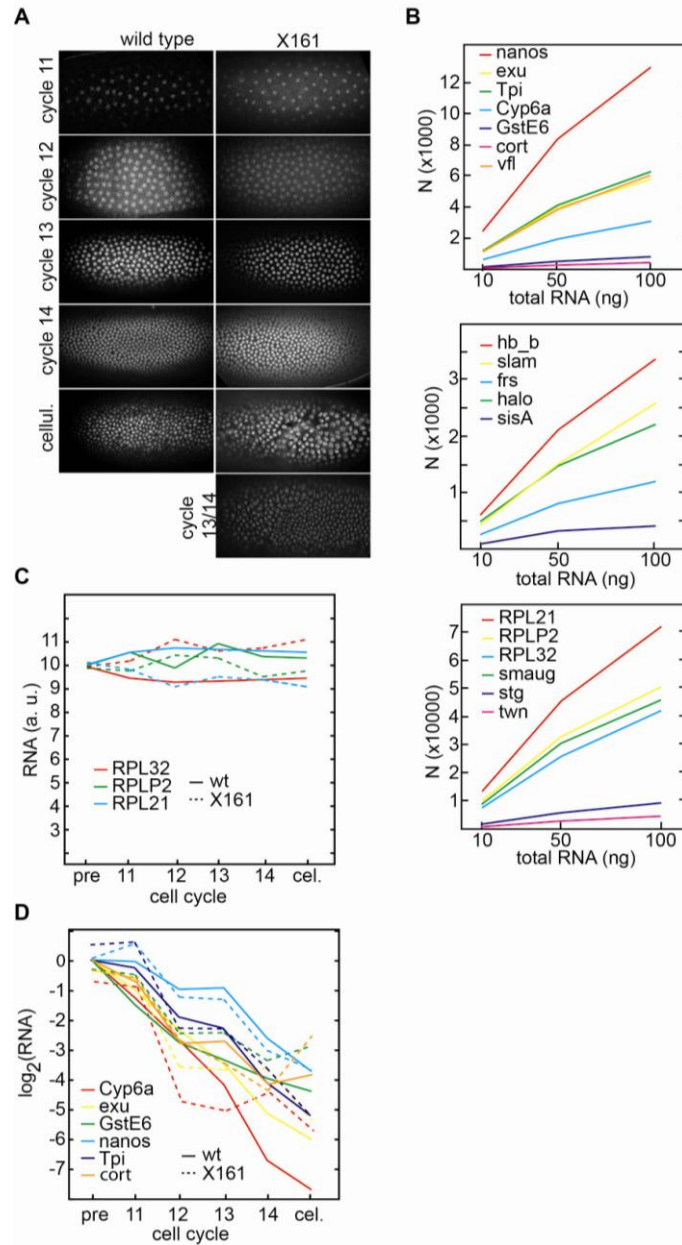


### Figure S3. Gene Expression Profiles by n-Counter NanoString

(A) Wild type and X161 embryos expressing Histone2Av-RFP were individually selected by their nuclear density. Images of embryos at indicated interphases and in cellularisation. X161 embryos in cellularisation were in interphase 13.

(B) Sensitivity of NanoString detection. Total RNA from wild type embryos of indicated stage was analysed for the amount of selected transcripts. Low abundant transcripts reached low readings at an input with 10 ng. Transcript levels in staged embryonic extracts measured by NanoString technology. Pre, presyncytal cycles 1-8. 11, 12, 13, 14, number of interphase. cel. embryos in cellularisation when the furrow is at the basal side of the nuclei in interphase 14 in wild type and interphase 13 in X161 embryos. (C and D) Pre, presyncytal cycles 1-8. 11, 12, 13, 14, number of interphase. cel. embryos in cellularisation when the furrow is at the basal side of the nuclei in interphase 14 in wild type and interphase 13 in X161 embryos. Transcript levels in wild type embryos are indicated by solid lines, in X161 embryos, by dashed lines. (C) Profiles of genes encoding ribosomal proteins. Y axis, log(2) scale. (D) Profiles of maternal genes, whose degradation depends on egg activation.

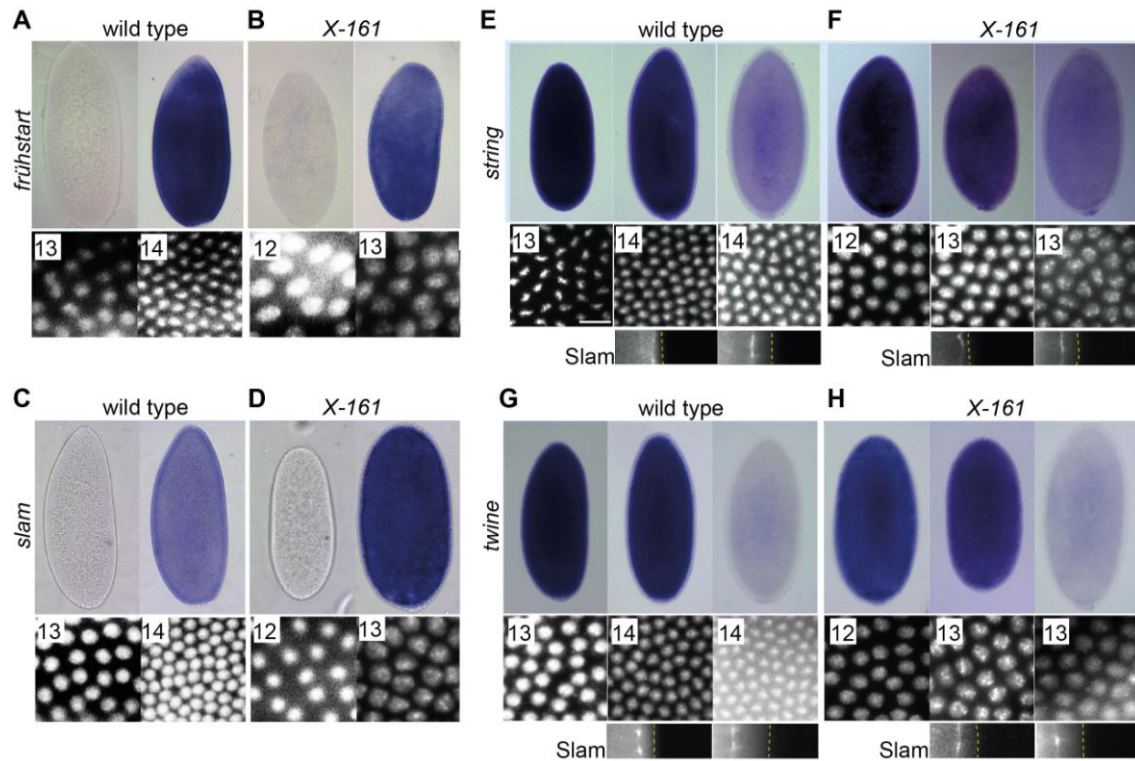


**Figure S4. Gene Expression by Whole Mount RNA In Situ Hybridization**

*frs* (A and B), *slam* (C and D), *string* (E and F), and *twine* (G and H) transcripts were detected by RNA in situ hybridisation (blue). The cell cycle number was determined by nuclear density as shown by DNA staining. The respective division cycle is indicated by the number in the inset. Progression of cellularization in cycle 14 in wild type and cycle 13 in mutants was determined by staining for Slam protein marking the cellularization front. The outline of the embryos is marked with a dashed yellow line.

**Table S1. Expression of *RPII215* by qPCR**

relative to 18S rRNA		Stage 1-2		Stage 4		Stage 5		Stage7-9	
		WT	X161	WT	X161	WT	X161	WT	X161
RPII215	mean	1,00	0,82	0,93	1,31	0,71	0,79	0,54	0,48
	SD	0,46	0,47	0,01	0,55	0,15	0,51	0,03	0,20
	P	0,73		0,44		0,85		0,71	
frs	mean	1,00	0,76	273,42	382,40	2834,07	2055,74	92,51	92,33
	SD	0,54	0,66	355,12	341,35	1433,84	2241,03	6,34	9,49
slam	mean	1,00	0,70	0,78	2,88	6,33	12,03	0,10	0,12
	SD	0,26	0,20	0,56	2,27	2,34	2,55	0,04	0,02

SD, standard deviation, P student T-test

**Table S2. Expression Levels by nCounter NanoString**

Type	Gene	wild type						X161					
		pre	11	12	13	14	cell	pre	11	12	13	14	cell13
stable	RPL32	14953,50	14121,50	13828,38	13939,76	14045,34	14153,00	14824,49	15256,74	16750,48	15884,20	16081,87	16746,20
stable	RpLP2	17868,66	18882,72	17589,41	19574,16	18527,97	18366,81	17525,11	17393,42	18611,99	18409,91	16812,82	17316,90
stable	Rpl21	25626,72	27136,56	27711,78	27490,36	27283,72	27076,17	25849,74	25117,37	22877,50	24125,17	23828,64	22883,35
zygotic expression	hb_a	19,94	84,26	174,22	511,23	1710,14	1829,58	15,19	152,09	1861,52	1523,56	1953,06	1724,88
zygotic expression	dpp	3,02	6,36	12,99	37,47	179,9	274,36	24,59	13,73	110,71	180,59	160,55	195,91
zygotic expression	sisA	44,11	178,05	184,92	244,13	316,86	779,46	53,52	176,38	1015,37	722,36	795,38	1090,29
zygotic expression	eve	7,25	38,15	85,58	183,7	349,43	867,46	9,4	119,35	455,49	373,9	417,23	1337,31
zygotic expression	halo	38,07	124,00	482,16	1065,97	5290,32	7835,25	50,63	157,37	3229,58	2780,05	7888,30	7683,15
zygotic expression	kni	2,42	6,36	16,05	31,42	274,66	545,03	22,42	10,56	143,92	132,26	223,93	587,74
zygotic expression	frs	11,48	39,74	238,88	397,62	4222,78	8096,30	10,13	32,74	2502,05	1465,06	7539,73	6618,41
zygotic expression	slam	198,82	329,07	246,81	569,24	2408,26	4451,93	372,47	458,39	2109,82	1627,84	2231,92	5093,71
zygotic degradation	smg	11662,46	17318,44	12135,84	15718,79	14325,92	5745,36	17190,97	22095,60	17359,38	18071,62	8626,64	1750,43
zygotic degradation	string	2185,16	3188,98	1966,10	2774,90	1931,49	574,61	4137,72	5852,38	3205,86	3517,67	795,38	370,53
zygotic degradation	twine	1440,06	1742,34	1414,40	1473,26	1513,21	911,83	1850,08	2226,46	2203,14	1699,06	1890,74	400,34
maternal degradation	cort	195,79	119,23	29,04	30,21	11,10	14,05	156,22	129,91	30,05	17,80	9,51	34,07
maternal degradation	Cyp6a19	2975,59	1247,93	456,95	164,37	28,13	14,05	1804,51	1587,46	110,71	89,02	136,26	55,37
maternal degradation	GstE6	219,36	77,90	32,09	21,75	14,07	10,35	177,92	156,32	39,54	40,70	21,13	29,81
maternal degradation	Nanos	4607,82	4502,09	2342,81	2409,91	755,87	343,88	4806,01	6768,10	1964,32	1838,96	567,22	362,01
maternal degradation	Tpi	2672,84	2233,56	712,17	555,95	157,69	72,47	3810,09	4086,42	551,97	546,85	220,76	72,40
maternal degradation	exu	3733,39	1869,51	735,09	333,57	106,61	56,94	2992,09	2483,11	313,15	289,96	304,21	89,44

Embryos were frozen 3 min after anaphase of the preceding mitosis. "Pre" were presyncytial embryos in nuclear cycle 1 to 8. "cell", "cell-13" were embryos in cellularisation when the furrow passed the basal side of the nuclei. For X161 embryos were in interphase 13. 50 ng of total RNA was analysed by NanoString nCounter technology according to the instructions of the manufacturer.

## Supplemental Experimental Procedures

### Genetics

Genetic markers, strains and genome annotation were according to Flybase, if not otherwise noted. X161 was selected from a set of mutations in germline clones with defects in oogenesis and early embryogenesis (1). For the genomic *RPII215* rescue construct a blunt SgrAI fragment from BAC clone CH321-136G02 into the blunt HpaI site of pCasper4. Transgenes were generated by standard procedures. Following mutations were employed *vfl*[294] (synonymous to *zld*[294]) (2), *grapes*[1] (3), *RPII215*[1], *RPII215*[G0040] (4, 5). Germline clones were induced with Frt[18E] or Frt[19A] and corresponding *ovoD* chromosomes by two heatshocks (each 1h, 37°C) to first and second instar larvae. Haploid embryos were generated by crossing females with *ms(3)K81* homozygous males (6). Transgenic fluorescent markers were Histone2Av-GFP/ mRFP and *sqh*-moesin-GFP (7).

### Microscopy

Cell cycle lengths were determined by time lapse recordings at about 21-23°C with an inverted Zeiss Axiovert microscope with differential interference contrast (Plan-apochromat 25xoil NA0.5). Fluorescent time lapses were recorded with a Zeiss spinning disc microscope with a Plan Neofluar 40xoil NA1.3 objective. Embryos were dechorionated with 50% bleach for 90s, washed with water, lined up and oriented on a piece of agarose, transferred to a coverslip and covered with halocarbon oil. Fixed and stained embryos were imaged with a Zeiss LSM780 microscope (LCI Plan-neofluar 25xmulti, NA 0.8C-apochromat 40xwater NA1.2, Plan-apochromat 63xoil NA 1.4). Images were processed with Fiji/ ImageJ.

### Histology

Embryos were dechorionated with 50% bleach, fixed for 20 min with 4% formaldehyde in PBS and stored in methanol at -20°C. For immunostaining rehydrated embryos were blocked with 5% BSA for 1 h, incubated with primary antibodies overnight at 4°C, washed for 1 h, incubated with secondary antibodies for 1 h, washed for 1 h, stained with DAPI (0.2 mg/l) and mounted in Aquapolymount (Polyscience). Staining/ washing buffer was PBS plus 0.1% Tween20. Following antibodies were used: CID (rabbit, ref. 8), Kugelkern (rabbit, guinea pig, ref. 9), Eve (guinea pig), gamma-Tubulin (GTU88, mouse, 0.2 mg/l, Sigma), Dlg (4F3, mouse, 0.4 mg/l, Hybridoma center), RNA polymerase II (clones ANA3 and H5, mouse, Millipore), Slam (rabbit, guinea pig, ref. 10), String (rabbit, S DiTalia), Twine (rat, obtained from S. DiTalia), Vfl (rat, ref. 11). The eve antibody (guinea pig) was raised against recombinant protein expressed from plasmid pAR-eve (obtained from M. Frasch). Secondary antibodies were alexa-coupled goat-anti-rabbit/ mouse/ guinea pig (4 mg/l, Invitrogen), alkaline phosphatase coupled anti-digoxigenin-Fab fragments (Roche). RNA in situ hybridisation was performed as previously described (12) using digoxigenin labelled probes and detection with alkaline phosphatase. Images were recorded with bright field optics. The RNA antisense probes were prepared from plasmids pCS2-frs, pNB-stg1.8, pSK-twine (24), pCS2-slam (10). For RNA-protein double staining, RNA staining was developed prior to immunostaining.

### Western Blots

Embryos were manually staged according to their morphology in bright field optics, collected in groups of 50 to 100 and frozen in liquid nitrogen. Proteins extracts were prepared by disruption of the embryos with a pistle fitting into a 1.5 ml reaction tube in Laemmli buffer. Protein extracts from about 5-10 embryos were separated by SDS polyacrylamid electrophoresis and transferred to PVDF membrane by wet transfer (110

mA, 4°C, 18hr). Following blocking with 5% non-fat milk in PBT (PBS plus 0.2% Tween20) overnight at 4°C the blot was incubated with primary antibody in PBT plus 1% bovine serum albumin for 2 h, washed with PBT (5x10 min), incubated with peroxidase coupled goat-anti-mouse antibody (Sigma) in PBT with 0.5% bovine serum albumin for 1 h, washed with PBT (5x5min) and developed with the enhanced chemiluminescence reaction (GE healthcare). Primary antibodies were alpha-Tubulin (B512, mouse, 0,04 mg/ l, Sigma), RNA polymerase II 215 subunit (ARNA-3a, H5 , mouse, 1:500, Millipore).

### **Quantitative PCR**

Embryos were manually staged according to their morphology in bright field optics, collected in groups of 50 to 100 and frozen in liquid nitrogen. Total RNAs was extracted with Trizol (Invitrogen) and analysed with a Bio analyzer (RNA 6000 Nano Kit, Agilent). cDNA was synthesised according to manufactor's instructions (Roche). In brief, 2 µg total RNA was mixed with 1 µM of oligo-dT and 8 µM of 18S rRNA specific primer (HS415 AAC ATG AAC CTT ATG GGA CGT GTG C) in 13 µl. The reaction was started by adding 7 µl with reverse transcriptase (1 unit), dNTP mix (each 1 mM), RNase inhibitor and buffer. For each real-time PCR reaction, cDNA corresponding to 10 ng of original total RNA was mixed with 3 µM of primers and reaction mix containing SyBR Green (iQ SYBR green supermix, Bio-RAD) with a CFX-96 real-time PCR system (Bio-RAD). The amplification curves were analyzed with the comparative CT method using either 18S rRNA as reference genes. The following primer pairs were used: RPII215: HS403 (GCG GTG GAT CGA CAC CGA GC) and HS404 (GCA CTT ACG TGG CCG GGT GG), RPL21: HS386(AGG CAT ATC ATG GCA AAA CC) and HS397 (GAC CCA TTG TCC CTT TTC CT), frs: HS375 (CTG ATC AGC CAG CCT AGC AG) and HS376 (TGT CCA GGG AGT AGC ACT CG). Slam: JG241 (GTG CAT CCA GCT GCA AGC AAT) and JG242 (CGG GCA TTG GAA GTG GGT TAC A), 18S rRNA: HS363 (AGC CTG AGA AAC GGC TAC CA) and HS364 (AGC TGG GAG TGG GTA ATT TAC G).

### **Expression Analysis by NanoString nCounter**

Single dechorionated embryos expressing Histone2Av-RFP were staged on a spinning disc microscope according to nuclear density and cell cycle stage. Embryos (five wild type, three mutant) of a given stage were pooled in vials with heptane on dry-ice. Presyncytial embryos were selected by morphology in bright field optics. Embryos in interphase 11 to 14 were frozen 3 min after anaphase. Embryos in cellularization were frozen when the furrow passed the basal side of the nuclear layer. Total RNA was extracted with Trizol (Invitrogen) and analysed by Bio-analyzer (RNA 6000 Nano Kit, Agilent). The yield was about 50 to 150 ng per embryo. Selected transcripts were quantified by NanoString technology (13) according to the protocol suggested by the manufacturer. Briefly, total RNA (50 ng) was mixed with the code set before adding the capture probe. Hybridization was performed at 65°C for 18 hr. Post-hybridization processing was performed with the nCounter Prep Station. After preparation, the cartridge containing the mRNAs were loaded into the Digital Analyzer and the number of RNA molecules was counted. The number of mRNA was analyzed by nSolver software. Data were corrected using *RPL21*, *RPL32* and *RPLP2* as reference genes.

### **Microinjection of Embryos**

Microinjection was performed as described as previously described (14).  $\alpha$ -amanitin was injected at 500 µg/ ml (in water) into presyncytial embryos expressing Histone2Av-RFP. Alexa488 labelled histone1 (2 mg/ ml) was injected into early embryos to visualise nuclear dynamics for the embryos *grapes* and X161; *grapes* (7).

## Supplemental References

1. Vogt, N., Koch, I., Schwarz, H., Schnorrer, F., Nüsslein-Volhard, C. (2006). The  $\gamma$ TuRC Components Grip75 and Grip128 Have an Essential Microtubule-Anchoring Function in the Drosophila Germline. *Development* 133, 3963–3972.
2. Liang, H. L., Nien, C. Y., Liu, H. Y., Metzstein, M. M., Kirov, N., Rushlow, C. (2008). The zinc-finger protein Zelda is a key activator of the early zygotic genome in Drosophila. *Nature* 456, 400-403.
3. Sibon, O. C., Stevenson, V. A., Theurkauf, W. E. (1997). DNA-replication checkpoint control at the Drosophila midblastula transition. *Nature* 388, 93-97.
4. Brinckey, W. J., Greenleaf, A. L. (1995). Functional studies of the carboxy-terminal repeat domain of Drosophila RNA polymerase II in vivo. *Genetics* 140, 599-613.
5. Meller, V. H., Rattner, B. P. (2002). The roX genes encode redundant male-specific lethal transcripts required for targeting of the MSL complex. *EMBO J* 21, 1084-1091.
6. Yasuda, G. K., Schubiger, G., Wakimoto, B. T. (1995). Genetic Characterization of ms(3)K81, A Paternal Effect Gene of Drosophila melanogaster. *Genetics* 140, 219-229.
7. Kanesaki, T., Edwards, C., Schwarz, U., Großhans, J. (2011). Dynamic ordering of nuclei in syncytial embryos: a quantitative analysis of the role of cytoskeletal networks. *Integ Biol* 3, 1112-1119
8. Jäger, H., Rauch, M., Heidmann, S. (2005). The Drosophila melanogaster condensin subunit Cap-G interacts with the centromere-specific histone H3 variant CID. *Chromosoma* 113, 350-61.
9. Brandt, A., Papagiannouli, F., Wagner, N., Wilsch-Bräuninger, M., Braun, M., Furlong, E. E., Loserth, S., Wenzl, C., Pilot, F., Vogt, N., Lecuit, T., Krohne, G., Großhans, J. (2006). Developmental control of nuclear size and shape by kugelkern and kurz kern. *Curr Biol* 16, 543-552.
10. Wenzl, C., Yan, S., Laupsien, P., Großhans, J. (2010). Localization of RhoGEF2 during Drosophila cellularisation is developmentally controlled by slam. *Mech Dev* 127, 371-384.
11. Liang, H. L., Nien, C. Y., Liu, H. Y., Metzstein, M. M., Kirov, N., Rushlow, C. (2008). The zinc-finger protein Zelda is a key activator of the early zygotic genome in Drosophila. *Nature* 456, 400-403.
12. Großhans, J., Müller, H. A., Wieschaus, E. (2003). Control of cleavage cycles in Drosophila embryos by frühstart. *Dev Cell* 5, 285-294.
13. Geiss, G. K., Bumgarner, R. E., Birditt, B., Dahl, T., Dowldar, N., Dunaway, D. L., Fell, H. P., Ferree, S., George, R. D., Grogan, T., James, J. J., Maysuria, M., Mitton, J. D., et al. (2009). Direct multiplexed measurement of gene expression with color-coded probe pairs. *Nature Biotech* 26, 317-325.
14. Großhans, J., Bergmann, A., Haffter, P., Nüsslein-Volhard, C. (1994). Activation of the protein kinase Pelle by Tube in the dorsoventral signalling cascade of Drosophila embryo. *Nature* 372, 563-566.